Event-driven Langevin simulations of hard spheres

A. Scala
ISC-CNR Dipartimento di Fisica, Sapienza Università di Roma Piazzale Moro 5, 00185 Roma, Italy,
IMT Alti Studi Lucca, piazza S. Ponziano 6, 55100 Lucca, Italy, and
London Institute of Mathematical Sciences, 22 South Audley St Mayfair, London W1K 2NY, United Kingdom
(Received 8 March 2012; revised manuscript received 11 July 2012; published 20 August 2012)

The blossoming of interest in colloids and nanoparticles has given renewed impulse to the study of hard-body systems. In particular, hard spheres have become a real test system for theories and experiments. It is therefore necessary to study the complex dynamics of such systems in presence of a solvent; disregarding hydrodynamic interactions, the simplest model is the Langevin equation. Unfortunately, standard algorithms for the numerical integration of the Langevin equation require that interactions are slowly varying during an integration time step. This is not the case for hard-body systems, where there is no clear-cut distinction between the correlation time of the noise and the time scale of the interactions. Starting first from a splitting of the Fokker-Plank operator associated with the Langevin dynamics, and then from an approximation of the two-body Green's function, we introduce and test two algorithms for the simulation of the Langevin dynamics of hard spheres.

DOI: 10.1103/PhysRevE.86.026709 PACS number(s): 05.10.Gg, 05.40.Jc

I. INTRODUCTION

Hard spheres (HS) are a reference system for structural and dynamical theories of fluids [1,2], but idealized: the infinitely steep potential is essentially a way of capturing the effects of steric interactions. On the atomic or the molecular scale, two-body interactions are mostly modeled by Lennard-Jones or Coulomb potentials; experiments on colloids shift the length scales of interest up to roughly 1 to 1000 nm where objects can behave as hard bodies and are still small enough to exhibit thermal or Brownian motion in a solvent. Dynamical light scattering [3,4] has already provided a rich collection of data for such systems, encouraging a considerable effort in understanding the dynamics; the possibility of following single particle trajectories via confocal microscopy of latex particle [5] has allowed a direct view on an experimental realization of HS systems and their dynamics [6,7].

The simplest model of a suspension of neutral particles is to consider a system of HS in an ideal solvent with no hydrodynamic interactions (HI); real suspensions are often described in terms of their deviations from such ideal systems. This is the most interesting (and the most studied) model for theoreticians, and many results have been derived: the two-body case (and hence the low density case) has been solved exactly [8,9] in the overdamped limit, while at moderate and high packing fractions various Enskog-type [10,11] or mode coupling theories [12,13] have been applied to understand the dynamics. While hydrodynamic interactions are well understood at low particle densities, much less is known at high densities, and theories often proceed by disregarding them [14]. As an example, theories regarding glass transition, such as mode coupling theory for Brownian hard spheres [13,15,16] or Brownian hard discs in shear flow [17], often neglect HI effects.

Even disregarding HI, such theories are not exact and to discriminate among them it is often necessary to resort to computer simulations. Non-HI simulations therefore have their place in testing such theories and circumvent the huge computational effort of the classical HI codes [18–21]. In order to validate non-HI theories for HS, it is necessary to use computer simulations, as only a qualitative agreement is to be expected among non-HI theories and data for real suspension. Standard simulation methods for Brownian dynamics such as the well-known Ermak-McCammon [22] require continuous potentials; to circumvent such a problem, several algorithms have been introduced with various degrees of justification [23–26] for the overdamped dynamics. Only recently, it has been recognized that in the case of hard interactions such simulations are better performed by event-driven (ED) codes [27–29].

For the overdamped dynamics, an entire class of event-driven algorithms based on the exact solution of first passage times and on the knowledge of two-body Green's function has been developed [30–33] (see [34] for a general review of the applications of ED dynamics to particle simulations); such algorithms are mostly designed to follow the reaction kinetics among particles, but are better tailored to work for systems at low packing fraction. As an example, to introduce hard-body collisions it would be necessary to implement numerically the solution of [8,9]; such a solution is not suitable for the fast numerical implementations necessary to simulate dense systems, as it consists of an infinite series of spherical harmonics in the Laplace domain.

In the case of the full Langevin dynamics, no solutions for the two-body Green's function are available, not even in one dimension. We introduce two new ED algorithms that go beyond the overdamped approximation and allow for the simulation of the full Brownian dynamics of HS; in doing so, by solving the problem of a Langevin particle in presence of an elastic wall, we introduce the solution of the one-dimensional two-body problem for the Langevin equation.

II. METHODS

We consider a system of N HS governed by the Langevin equation

$$\begin{aligned} \partial_t \mathbf{v}_i &= -\gamma \mathbf{v}_i + \mathbf{a}_i + \boldsymbol{\xi}_i, \\ \partial_t \boldsymbol{r}_i &= \mathbf{v}_i \end{aligned} \tag{1}$$

for the positions $\mathbf{r}_i$ and the velocities $\mathbf{v}_i$; here, γ is the friction constant, $\mathbf{a}_i = -m^{-1}\partial_{\mathbf{r}}U$ the acceleration, m is the mass of the HS, U is the potential energy, and $m\boldsymbol{\xi}_i$ are the zero-mean random forces due to the solvent. We assume that such random forces are delta correlated and satisfy the fluctuation-dissipation theorem

$$\langle \boldsymbol{\xi}_i(\mathbf{x},t) \otimes \boldsymbol{\xi}_j(\mathbf{x}',t')\rangle = \gamma \frac{2k_BT}{m}\delta(\mathbf{x}-\mathbf{x}')\delta(t-t')\delta_{ij}\mathbf{1}. \quad (2)$$

In the case of continuous interactions, it is possible to define stochastic Taylor expansions [35]; correspondingly, integration schemes of the kth order with errors of order $(\Delta t)^k$ in the time step Δt can be introduced [36]. In the case of hard-body interactions, all the standard machinery of stochastic calculus breaks down due to the singular nature of the interaction potential and new methods must be developed.

We consider the Fokker-Plank equation associated to the stochastic differential equation (SDE) (1) (Kramers' equation [37])

$$\partial_t W = \mathbf{L}_K W, \quad (3)$$

where $W(\mathbf{r},\mathbf{v},t)$ is the probability distribution function (PDF) for the positions $\mathbf{r} = \{\mathbf{r}_i\}$ and the velocities $\mathbf{v} = \{\mathbf{v}_i\}$ of the particles, $v_{th}^2 = k_BT/m$ relates to the temperature, and

$$\mathbf{L}_K = \gamma\left(\partial_{\mathbf{v}}\cdot\mathbf{v} + v_{th}^2\partial_{\mathbf{v}}^2\right) - (\mathbf{v}\cdot\partial_{\mathbf{r}} + \mathbf{a}\cdot\partial_{\mathbf{v}}) \quad (4)$$

is the Kramer operator. Integrating the SDE (1) for a finite time step Δt corresponds to extracting a configuration $\{\mathbf{r}^{t+\Delta t},\mathbf{v}^{t+\Delta t}\}$ according to the probability $e^{\mathbf{L}_K\Delta t}\delta(\mathbf{x}-\mathbf{x}^t,\mathbf{v}-\mathbf{v}^t)$.

III. SPLIT BROWNIAN DYNAMICS

To obtain a numerical approximation, a powerful approach is to split the evolution operator $e^{\mathbf{L}_K\Delta t}$ in a product $e^{\mathbf{L}_K\Delta t} \approx \prod_i e^{a_i\mathbf{L}_i\Delta t}$ of exactly integrable operators $\mathbf{L}_i$ [38], ensuring that the decomposition is positive (i.e., all $a_i > 0$) [39]. Therefore, to each splitting corresponds an algorithm in which in a single time step Δt, the operators $e^{a_i\mathbf{L}_i\Delta t}$ are applied in sequence. We first choose to split $\mathbf{L}_K$ into the reversible (or streaming) operator $\mathbf{L}_{\rm rev} = -(\mathbf{v}\cdot\partial_{\mathbf{r}} + \mathbf{a}\cdot\partial_{\mathbf{v}})$ and the irreversible (or collision) operator $\mathbf{L}_{\rm irr} = \gamma(\partial_{\mathbf{v}}\cdot\mathbf{v} + v_{th}^2\partial_{\mathbf{v}}^2)$ [40]; we indicate the corresponding algorithm as split Brownian dynamics (SBD).

The operator $\mathbf{L}_{\rm rev}$ is the Liouvillian associated to the Hamiltonian $\mathcal{H} = m\,\mathbf{v}\cdot\mathbf{v}/2 + U$. In the case of step potentials, the associated reversible equation of motion can be integrated via event-driven molecular dynamics (EDMD) [41] with a precision limited only by the numerical round-off errors; therefore, the propagator $e^{\mathbf{L}_{\rm rev}\Delta t}$ can be implemented with extreme accuracy.

The operator $\mathbf{L}_{\rm irr}$ corresponds to the interaction with the bath; the associated SDE $\partial_t\mathbf{v} = -\gamma\mathbf{v} + \xi$ can be exactly integrated giving an explicit formula for the evolution $\mathbf{v}^{t+\Delta t} = e^{\mathbf{L}_{\rm irr}\Delta t}\mathbf{v}^t$:

$$\mathbf{v}_{i,\alpha}^{t+\Delta t} = e^{-\gamma\Delta t}\mathbf{v}_{i,\alpha}^t + \sqrt{v_{th}^2(1-e^{-2\gamma\Delta t})}\Gamma, \quad (5)$$

where Γ is a unitary Gaussian random variable and $\alpha \in \{x,y,z\}$; such a solution can be obtained either by straightforward Ito integration of the Langevin equation for the free particle or via more elegant operatorial methods [42].

The algorithm for the single SBD time step $e^{\mathbf{L}_{\rm rev}\Delta t}e^{\mathbf{L}_{\rm irr}\Delta t}$ consists therefore in an EDMD simulation [41] of length Δt followed by a thermalization of the velocities according to Eq. (5). We notice that the error is at most quadratic [as can be checked via Taylor expansion $e^{\mathbf{L}_{\rm rev}\Delta t}e^{\mathbf{L}_{\rm irr}\Delta t} = e^{\mathbf{L}_K\Delta t} + O(\Delta t^2)$] *and regards only in the dynamics*; in fact, SBD is equivalent [upon identifying the angle α mixing reversible and irreversible evolution with $\cos(\alpha) = e^{-\gamma(t-t')}$] to the generalized hybrid Monte Carlo [43] and therefore explores the canonical ensemble as long as the propagation steps $e^{\mathbf{L}_{\rm rev}\Delta t}$, $e^{\mathbf{L}_{\rm irr}\Delta t}$ can be exactly implemented (as in our case). Notice that Eq. (5) tell us that performing SBD simulations is equivalent to thermalize periodically ED molecular dynamics of hard spheres with a Grest-Kremer thermostat [44]; in the limit of $\gamma\Delta t \gg 1$, Eq. (5) reduces to the well known Andersen thermostat [45].

It is therefore of interest to give some physical bounds on the magnitude of the feasible time step Δt. First, we notice that for $\Delta t \to \infty$, the dynamics reduces to MD simulations where velocities are extracted each Δt from a Maxwellian; therefore, if the time step is much bigger than the average interparticle collision time, results of classical MD are to be expected. Accordingly, we find that for big Δt the algorithm overestimates the diffusion coefficient (Fig. 1); this is to be expected as the mean-free path (in absence of collisions) of a particle is of order $v_{th}\Delta t$ instead of $\gamma^{-1}v_{th}\sqrt{\Delta t}$. Second, we notice that the damping γ introduces a natural time scale $\tau = \gamma^{-1}$ that can be thought to measure the frequency of the interaction with the thermal bath. As the SBD introduces an interaction with the bath at each time step, it is natural to require $\Delta t < \tau$. Accordingly, we find that SBD overestimates diffusion coefficients for $\Delta t \gtrsim \gamma^{-1}$ (Fig. 1); in particular,

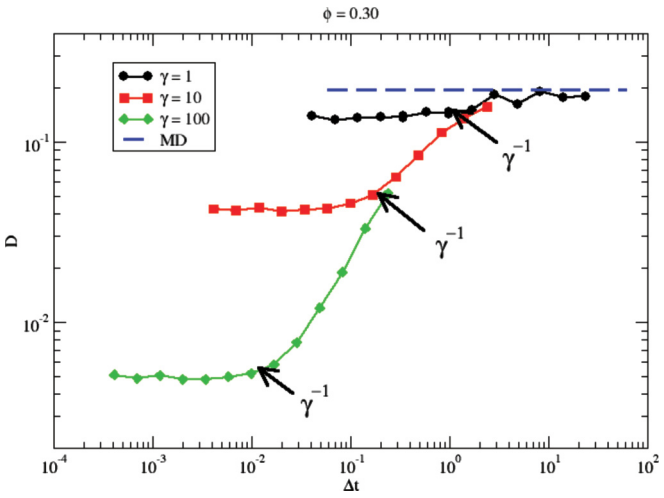

FIG. 1. (Color online) Effect of the damping coefficient γ on the size of the simulation step Δt (all quantities in reduced units). The diffusion coefficient D from simulations is plotted versus the time-step size Δt for various γ's. As expected, the system approaches the MD value for diffusion regardless of γ for $\Delta t \to \infty$. The "true" value of D is obtained for $\Delta t \to 0$. We observe at small Δt's a plateau in the D vs Δt plot for $\Delta t \lesssim \gamma^{-1}$, signaling that the "true" value of D is approached. Results are presented for packing fraction $\phi = 0.30$; a completely analogous behavior is found at a low packing fraction $\phi = 0.10$ and a high packing fraction $\phi = 0.45$.

for $\Delta t \gg \gamma^{-1}$, SBD recovers the Newtonian results and the simulation becomes equivalent to an NVT molecular dynamics interaction with an Andersen thermostat [45]. Thus, SBD is not well indicated for simulations in the overdamped limit $\gamma/m \to \infty$ and it is therefore necessary to develop an alternative approach for the simulation of systems with high damping.

IV. APPROXIMATE GREEN'S FUNCTION DYNAMICS

The best code for overdamped BD is the event-driven first-passage kinetic Monte Carlo algorithm [31–33], which does not require any pairwise or small enough time-step approximations; nevertheless, it has no straightforward extension to the full Langevin case. We will rely instead on the algorithm of [29], that also allows us to simulate Eq. (1) in the overdamped limit by using ED codes. The algorithm relies on considering time steps Δt small enough so that mostly binary collisions are relevant, i.e., the average displacement should be less than the average interparticle separation. Moreover, average displacement should be smaller than the HS radii in order to map the interaction of two nearby HS in the problem of a random walk near a reflective wall. Under such approximations, the true two-body stochastic dynamics for overdamped Brownian HS can be implemented by an algorithm of [29] in which each step consists in predicting the displacements $\Delta\mathbf{x}$ of the HS via the free propagator, introducing fictive velocities $\mathbf{v}^f = \Delta\mathbf{x}/\Delta t$, and performing an EDMD with such fictive velocities during t and $t + \Delta t$. We extend such approach to the general Brownian case.

First, we need to predict the positions of the HS after a time step Δt according to their free propagation, i.e., the solution of Eq. (1) with no interaction ($\mathbf{a} = 0$):

$$\begin{aligned} \mathbf{v}^0(t+\Delta t) &= \mathbf{v}^0(t) + \Delta\mathbf{v}^0 = \mathbf{v}^0(t) + \overline{\Delta\mathbf{v}^0} + \Delta\mathbf{v}^0_R, \\ \mathbf{r}^0(t+\Delta t) &= \mathbf{r}^0(t) + \Delta\mathbf{r}^0 = \mathbf{r}^0(t) + \overline{\Delta\mathbf{r}^0} + \Delta\mathbf{r}^0_R. \end{aligned} \tag{6}$$

The particle displacements contain both systematic parts $\overline{\Delta\mathbf{v}^0} = (e^{-\gamma t} - 1)\,\mathbf{v}^0(t)$, $\overline{\Delta\mathbf{r}^0} = \gamma^{-1}(1 - e^{-\gamma t})\,\mathbf{v}^0(t)$ and stochastic displacements. The stochastic displacements $\Delta\mathbf{v}^0_R$, $\Delta\mathbf{r}^0_R$ are zero-mean correlated Gaussian variables with variances $\langle \| \Delta\mathbf{v}^0_R \|^2 \rangle = m^{-1}k_BT\,(1 - e^{-2\gamma t})$, $\langle \| \Delta\mathbf{r}^0_R \|^2 \rangle = \gamma^{-1}m^{-1}k_BT\,[2t - \gamma^{-1}(3 + 4e^{-\gamma t} + e^{-2\gamma t})]$ and cross correlation $\langle \Delta\mathbf{r}^0_R \Delta\mathbf{v}^0_R \rangle = \gamma^{-1}m^{-1}k_BT\,(1 - e^{-\gamma t})^2$ [46].

If we consider a time step such that the average displacement is less than the average interparticle separation, we can consider only the corrections due to two-body interactions. In the limit of small Δt, a couple of HS will interact only when they start from nearby positions. In particular, if $\gamma^{-1} v_{th}\sqrt{\Delta t} \ll \sigma$, i.e., the average free displacement is much smaller than the diameter σ of the HS, the dynamics of two particles A and B can be approximated as the Langevin dynamics of a point particle at a distance $(\mathbf{r}_A - \mathbf{r}_B)(1 - \sigma/\|\mathbf{r}_A - \mathbf{r}_B\|)$ from a flat wall. It is possible to solve such a problem with a straightforward generalization of the image method applied in [29]. In fact, the solution given by the free particle Green's function plus an image particle with a reflected velocity beyond the reflective wall (Fig. 2) correctly satisfies the zero-current boundary condition $\widehat{\mathbf{n}} \cdot \mathbf{j}|_{\text{wall}} = 0$, where $\widehat{\mathbf{n}}$ is the normal to the wall and $\mathbf{j}(\mathbf{r},t) = \int \mathbf{v} W(\mathbf{r},\mathbf{v},t) d\mathbf{v}$ is the probability current for the position.

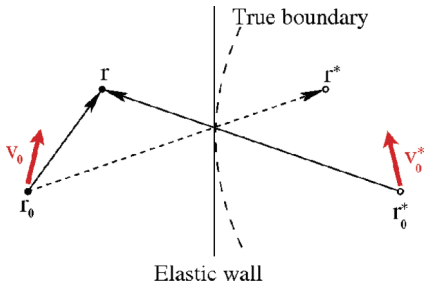

FIG. 2. (Color online) A two-body problem for hard spheres can be mapped into the problem of a point particle interacting with a larger sphere. When particles are very near, the problem further simplifies to the interaction of a Langevin particle with a reflective flat wall, the solution of which can be derived by applying the image method to the Langevin equation. In fact, the Green's function must be zero inside the wall and must satisfy the no-flux boundary conditions at the wall. Combining the free Green's function of the particle in its initial position and the free Green's function of its image (with the normal-to-the-wall component of the initial velocity reflected) satisfies both Kramers' equations and reflective boundary conditions giving the correct solution.

Such a solution can be implemented exactly by predicting the new positions and velocities $\mathbf{r}^0(t + \Delta t)$, $\mathbf{v}^0(t + \Delta t)$ according to Eq. (6), defining fictive velocities $\mathbf{v}^f = [\mathbf{r}^0(t + \Delta t) - \mathbf{r}^0(t)]/\Delta t$ and performing an EDMD simulation with such fictive velocities during Δt; if a collision happens, the component of the relative velocity normal to the contact point must be reflected for both the fictive $\mathbf{v}^f$ and the predicted velocities $\mathbf{v}^0(t + \Delta t)$. We indicate such algorithm as the approximate Green's function dynamics (AGD). In the overdamped limit, the prediction of the velocities and positions decorrelates and the algorithm correctly reduces to the overdamped case of [29]. The core of the algorithm is the collision among two particles i and j during a time step Δt and can be implemented as follows:

(1) Extract the free displacements $\Delta\mathbf{r}^0_i$, $\Delta\mathbf{r}^0_j$ and the putative final velocities $\mathbf{v}^0_i$, $\mathbf{v}^0_j$ according to Eq. (6).

(2) Define the fictive velocities $\mathbf{v}^f_i = \Delta\mathbf{r}^0_i/\Delta t$, $\mathbf{v}^f_j = \Delta\mathbf{r}^0_j/\Delta t$.

(3) Calculate the fictive collision time $t_c \in [0, \Delta t]$, and the normal $\hat{\sigma}^*_{ij}$ between the two spheres at contact at time t_c.

(4) Calculate the fictive post-collision velocities $\mathbf{v}^{f*}_i = \mathbf{v}^f_i - 2(\hat{\sigma}^*_{ij} \cdot \mathbf{v}^f_{ij})\hat{\sigma}^*_{ij}$ and $\mathbf{v}^{f*}_j = \mathbf{v}^f_j + 2(\hat{\sigma}^*_{ij} \cdot \mathbf{v}^f_{ij})\hat{\sigma}^*_{ij}$ with $\mathbf{v}^f_{ij} = \mathbf{v}^f_i - \mathbf{v}^f_j$.

(5) Calculate the final positions $\mathbf{r}_i(t + \Delta t) = \mathbf{r}_i(t) + \mathbf{v}^f_i \cdot t_c + \mathbf{v}^{f*}_i \cdot (\Delta t - t_c)$ and $\mathbf{r}_j(t + \Delta t) = \mathbf{r}_j(t) + \mathbf{v}^f_j \cdot t_c + \mathbf{v}^{f*}_j \cdot (\Delta t - t_c)$.

(6) Calculate the final velocities $\mathbf{v}_i(t + \Delta t) = \mathbf{v}^0_i - 2(\hat{\sigma}^*_{ij} \cdot \mathbf{v}^0_{ij})\hat{\sigma}^*_{ij}$ and $\mathbf{v}_j(t + \Delta t) = \mathbf{v}^0_j + 2(\hat{\sigma}^*_{ij} \cdot \mathbf{v}^0_{ij})\hat{\sigma}^*_{ij}$ with $\mathbf{v}^0_{ij} = \mathbf{v}^0_i - \mathbf{v}^0_j$.

As for the SBD algorithm, it can be proven that the AGD scheme respects detailed balance and ergodicity and therefore explores the correct ensemble for HS; hence, errors are again only in dynamic quantities. At difference with SBD, we have

no analytic estimate for the error; nevertheless, we expect that the the mean-free path in absence of collisions $\gamma^{-1}v_{th}\sqrt{\Delta t}$ must be smaller than the radius of the HS in order to satisfy the flat-wall approximation, and must be smaller than the average interparticle distance in order to reduce the frequency of multiple collision (i.e., the fact that a single particle suffers more than a collision during Δt); in fact, the algorithms do not account for effects higher than two-body collisions and hence multiple collisions introduce further errors in the evaluation of dynamical quantities.

In order to check that the behavior of AGD is driven just by geometrical considerations, we have simulated HS systems at different γ and ϕ varying the time step Δt in the range $[10^{-2},10^{0}]$ (reduced units). At difference with SBD where

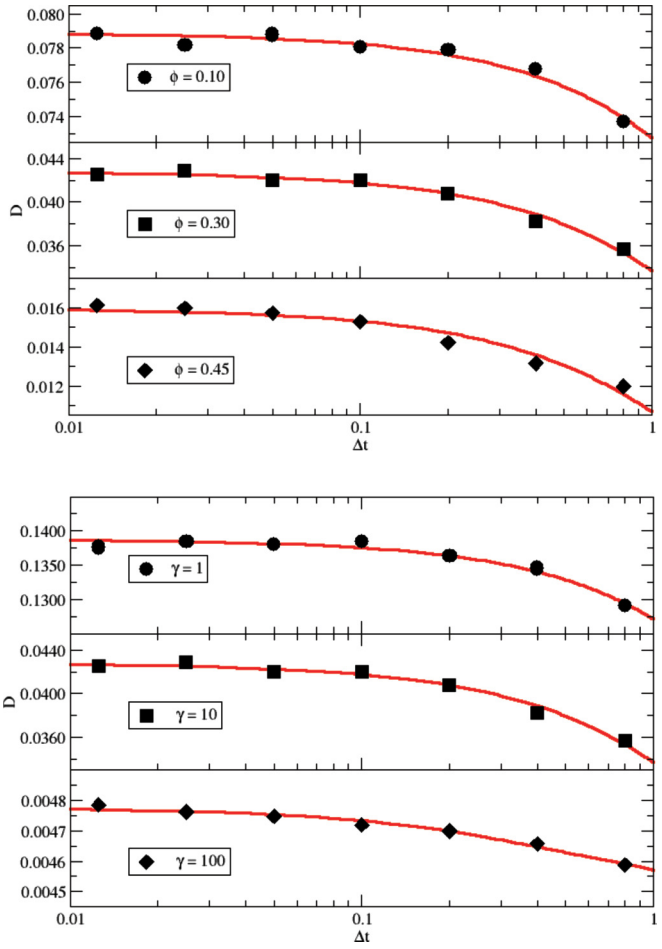

FIG. 3. (Color online) Effects of packing fraction ϕ (upper panel) and of the damping coefficient γ (lower panel) on the time step Δt for the AGD algorithm. All quantities in reduced units; thick lines are just a guide for the eye. Diffusion D is calculated averaging over 10 independent trajectories for 2000 particle systems; simulations are long at least 10 times the structural correlation time. In the upper panel, results are shown for $\phi = 0.10,0.30,0.45$ at fixed damping $\gamma = 10$. In the lower panel, results are shown for $\gamma = 1,10,100$ at fixed packing fraction $\phi = 0.30$. Notice that the estimated diffusion coefficient D has a small relative variation in the wide range of dampings γ's and packing fractions ϕ's analyzed. As a rule of thumb, to estimate D with an accuracy much smaller than 1% time step of order $\Delta t \sim 0.1$ is already enough.

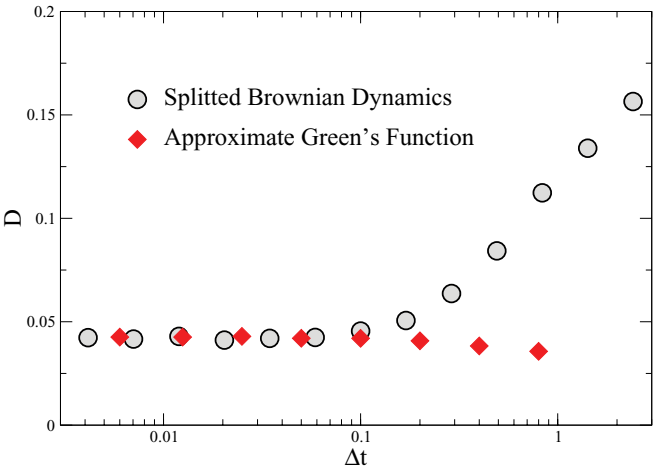

FIG. 4. (Color online) Comparison of the convergence of the measured diffusion coefficient D for the two algorithms considered in the papers. The figure shows results for damping $\gamma = 10$ at packing fraction $\phi = 0.30$ at varying time steps Δt; within the numerical accuracy (size of the symbols is of the order of the error), both algorithms converge to the same value for $\Delta t \to 0$. An analogous behavior is observed for $\phi = 0.10,0.45$ and $\gamma = 1,100$.

diffusion can vary even by a order of magnitude in such a Δt range, the values of D measured from AGD vary a few percent over the range and long simulations are necessary to have enough statistics to detect the behavior of D that would otherwise look flat. In Fig. 3, we show that the measured diffusion coefficient D versus the AGD simulation time step displays a plateau (i.e., fluctuations become much smaller than 1%) already for $\Delta t \lesssim 0.1$ regardless of γ and ϕ.

To better compare the two algorithms, we show in Fig. 4 the behavior of the measured diffusion coefficient D with respect to the time step Δt for $\phi = 0.30$, $\gamma = 0.10$. In the limit $\Delta t \to 0$, SBD becomes exact and the measured D tends to the theoretical D apart from the intrinsic numerical truncation errors; Fig. 4 shows how AGD approaches the same value with smaller errors at larger time steps. The same qualitative behavior is found at high and low density ($\phi = 0.10,0.45$) and high and low damping ($\gamma = 1,100$).

V. CONCLUSIONS

Hard spheres, and in general hard-body systems in suspension, have become a realistic model due to the developments of experimental techniques for the investigation of colloidal systems and nanoparticles, yet the dynamics of such systems is hard to simulate via the standard Brownian dynamics algorithms. In fact, classical continuous-time algorithms fail due to instantaneous character of the interactions; we have shown instead how it is possible to simulate the full Langevin dynamics of hard spheres.

First, we have shown how the simplest splitting of the stochastic evolution operator (a technique often referred to as "Trotterization" from Trotter's seminal work [47]) allows us to write an algorithm [the split Brownian dynamics (SBD)]. The SBD algorithm becomes inefficient of high viscosities, but the operator-splitting technique, by separating the deterministic motion from the interaction with the noise, could easily

take account for the interaction with external fields or with the presence of fluxes (such as shear) in the surrounding fluid. In fact, event-driven molecular dynamics algorithms can take account both for constant fields (a simple modification of the collision time predictor is required) and for shear (via Lees-Edwards boundary conditions) [41]. Notice that for small time steps, one could also simulate particles in varying fields as long as they can be considered constant during Δt.

Second, we have shown how by considering the two-body dynamics of Brownian hard spheres it is possible to develop an algorithm [the approximate Green's function dynamics (AGD)] that overcomes such a problem and works equally well for a wide range of packing fractions and viscosities. To develop the AGD algorithm, we have solved the problem of the Langevin dynamics $\partial_t v = -\gamma v + \xi$ of a point particle in presence of a reflective wall by extending the classical image method solution for the overdamped Brownian dynamics $\partial_t x = \eta$ of a point particle in presence of a reflective wall (here, ξ, η are noises). The AGD algorithm is event driven and considers fictive collisions between hard spheres. While it should possible to take into account the polydispersity of a system by considering also effective masses in the fictive collisions as hinted in [29], including shear or external fields in the AGD algorithm looks more complicated as it would require the solution of the particle-reflective wall problem with external fields or shear [48,49].

Both SBD and AGD simulations explore the canonical ensemble for hard spheres and therefore reproduce the correct equilibrium thermodynamics. They belong to the class of asynchronous event-driven particle algorithms [50] and can be easily implemented by adapting existing codes for ED dynamics [41] or Brownian dynamics [51] of hard spheres.

ACKNOWLEDGMENTS

The author thanks Th. Voigtmann for his hospitality at the physics department of Konstanz and for the long, useful discussions. The author acknowledges the support of the CNR-PNR National Project Crisis-Lab.

[1] H. C. Andersen, J. D. Weeks, and D. Chandler, Phys. Rev. A **4**, 1597 (1971).
[2] J. P. Hansen and I. R. McDonald, *Theory of Simple Liquid*, 2nd ed. (Academic, New York, 1989).
[3] B. J. Berne and R. Pecora, *Dynamic Light Scattering: with Applications to Chemistry Biology, and Physics* (Wiley, New York, 1976).
[4] V. D. Giorgio, M. Corti, and M. e. Giglio, *Light Scattering in Liquids and Macromolecular Solutions* (Plenum, New York, 1980).
[5] A. van Blaaderen and P. Wiltzius, Science **270**, 1177 (1995).
[6] W. K. Kegel and A. van Blaaderen, Science **287**, 290 (2000).
[7] E. R. Weeks, J. C. Crocker, A. Levitt, A. C. Schofield, and D. A. Weitz, Science **287**, 627 (2000).
[8] S. Hanna, W. Hess, and R. Klein, Phys. A (Amsterdam) **111**, 181 (1982).
[9] B. J. Ackerson and L. Fleishman, J. Chem. Phys. **76**, 2675 (1982).
[10] B. U. Felderhof and R. B. Jones, Phys. A (Amsterdam) **121**, 329 (1983).
[11] B. Cichocki and B. U. Felderhof, Phys. Rev. A **42**, 6024 (1990).
[12] W. Hess and R. Klein, Adv. Phys. **32**, 173 (1983).
[13] M. Fuchs and M. E. Cates, Phys. Rev. Lett. **89**, 248304 (2002).
[14] B. U. Felderhof and R. B. Jones, Faraday Discuss. Chem. Soc. **76**, 179 (1983).
[15] J. M. Brader, T. Voigtmann, M. E. Cates, and M. Fuchs, Phys. Rev. Lett. **98**, 058301 (2007).
[16] J. M. Brader, M. E. Cates, and M. Fuchs, Phys. Rev. Lett. **101**, 138301 (2008).
[17] O. Henrich, F. Weysser, M. E. Cates, and M. Fuchs, Philos. Trans. R. Soc. London A **367**, 5033 (2009).
[18] J. F. Brady and G. Bossis, Annu. Rev. Fluid Mech. **20**, 111 (1988).
[19] R. Adhikari, K. Stratford, M. E. Cates, and A. J. Wagner, Europhys. Lett. **71**, 473 (2005).
[20] R. D. Groot and P. B. Warren, J. Chem. Phys. **107**, 4423 (1997).
[21] H. Tanaka and T. Araki, Phys. Rev. Lett. **85**, 1338 (2000).
[22] D. L. Ermak and J. A. McCammon, J. Chem. Phys. **69**, 1352 (1978).
[23] B. Cichocki and K. Hinsen, Phys. A (Amsterdam) **166**, 473 (1990).
[24] D. M. Heyes and J. R. Melrose, J. Non-Newtonian Fluid Mech. **46**, 1 (1993).
[25] W. Schaertl and H. Sillescu, J. Stat. Phys. **74**, 687 (1994).
[26] D. R. Foss and J. F. Brady, J. Fluid Mech. **407**, 167 (2000).
[27] P. Strating, Phys. Rev. E **59**, 2175 (1999).
[28] Y.-G. Tao, W. K. den Otter, J. K. G. Dhont, and W. J. Briels, J. Chem. Phys. **124**, 134906 (2006).
[29] A. Scala, C. De Michele, and T. Voigtmann, J. Chem. Phys. **126**, 134109 (2007).
[30] T. M. A. O. M. Barenbrug, E. A. J. F. F. Peters, and J. D. Schieber, J. Chem. Phys. **117**, 9202 (2002).
[31] T. Oppelstrup, V. V. Bulatov, G. H. Gilmer, M. H. Kalos, and B. Sadigh, Phys. Rev. Lett. **97**, 230602 (2006).
[32] T. Oppelstrup, V. V. Bulatov, A. Donev, M. H. Kalos, G. H. Gilmer, and B. Sadigh, Phys. Rev. E **80**, 066701 (2009).
[33] A. Donev, V. V. Bulatov, T. Oppelstrup, G. H. Gilmer, B. Sadigh, and M. H. Kalos, J. Comput. Phys. **229**, 3214 (2010).
[34] A. Donev, Simulation **85**, 229 (2009).
[35] D. Kannan and V. Lakshmikantham, *Handbook of Stochastic Analysis and Applications* (Marcel Dekker, New York, 2002), Chap. 5.
[36] P. E. Kloeden and E. Platen, *Numerical Solution of Stochastic Differential Equations*, 3rd ed., Applications of Mathematics, Vol. 23 (Springer, Berlin, 1999).
[37] H. Kramers, Physica (Amsterdam) **7**, 284 (1940).
[38] H. A. Forbert and S. A. Chin, Phys. Rev. E **63**, 016703 (2000).
[39] S. A. Chin, Phys. Rev. E **71**, 016703 (2005).

[40] H. Risken, *The Fokker-Planck Equation. Methods of Solution and Applications*, 2nd ed. (Springer Series in Synergetics) (Springer, Berlin, 1989).
[41] D. C. Rapaport, *The Art of Molecular Dynamics Simulation* (Cambridge University Press, Cambridge, UK, 2004).
[42] M. Beccaria and G. Curci, Phys. Rev. D **49**, 2578 (1994).
[43] A. D. Kennedy, Parallel Computing **7**, 284 (1999).
[44] G. S. Grest and K. Kremer, Phys. Rev. A **33**, 3628 (1986).
[45] H. C. Andersen, J. Chem. Phys. **72**, 2384 (1980).
[46] M. P. Allen and D. J. Tildesley, *Computer Simulation of Liquids*, 2nd ed. (Clarendon, Oxford, 1987).
[47] H. F. Trotter, Proc. Am. Math. Soc. **10**, 545 (1959).
[48] M. V. Smoluchowsky, Z. Phys. **17**, 557 (1916); **17**, 585 (1916).
[49] A. Scala, arXiv:1207.0531.
[50] A. Donev, Simulation **85**, 229 (2009).
[51] A. Scala, http://gna.org/projects/hardbrown.